Robust Proton Conduction against Mechanical Stress in Flexible Free-Standing Membrane Composed of Two-Dimensional Coordination Polymer

Jiangfeng Lu, Yukihiro Yoshida*, Kazuyoshi Kanamori, Hiroshi Kitagawa*

[*] Jiangfeng Lu, Prof. Yukihiro Yoshida, Dr. Kazuyoshi Kanamori, Prof. Hiroshi Kitagawa
Division of Chemistry, Graduate School of Science, Kyoto University, Kitashirakawa-Oiwakecho, Sakyo-ku, Kyoto 606-8502(Japan)
E-mail: yoshiday@ssc.kuchem.kyoto-u.ac.jp; kitagawa@kuchem.kyoto-u.ac.jp

Supporting information for this article is given via a link at the end of the document.

Abstract: Introduction of mechanical flexibility into proton-conducting coordination polymers (CPs) is in high demand for future protonic applications such as fuel cells and hydrogen sensors. Although such mechanical properties have been primarily investigated in one-dimensional (1D) CPs, in this study, we successfully fabricated highly flexible free-standing CP membranes with a high surface-to-volume ratio, which is beneficial for enhanced performance in the aforementioned applications. We fabricated a layered CP, Cu_2(NiTCPP) (H_4(H_2TCPP); 5,10,15,20-tetrakis(4-carboxyphenyl)porphyrin), in which a two-dimensional (2D) square grid sheet composed of tetradentate nickel porphyrins and paddlewheel-type copper dimers was connected to each other by weak van der Waals forces. The mechanical flexibility was evaluated by bending and tensile tests. The flexural and Young's moduli of the membrane were significantly higher than those of conventional Nafion membranes. Electrochemical impedance spectroscopy analysis revealed that the in-plane proton conductivity of the membrane was maintained even under applied bending stress. Because the X-ray diffraction analysis indicates that the proton-conducting pathway through the hydrogen bonding network remains intact during the bending operation, our present study provides a promising strategy for the fabrication of new and advanced 2D CPs without using substrates or additional polymers for protonic devices.

Porous coordination polymers (PCPs) are crystalline materials formed by the self-assembly of metal ions/clusters with organic linkers via coordination bonds.[1] Because the judicious selection of components can control the surface potential (i.e., hydrophilicity/hydrophobicity and Lewis acidity/basicity) and geometrical structure of the pore spaces, PCPs provide a versatile platform for proton conduction when Lewis acidic molecules (e.g., phosphoric acid) or Lewis basic molecules (e.g., water) are accommodated in the pores.[2] Therefore, PCPs have great potential for protonic applications, such as proton exchange membrane fuel cells,[3] proton field-effect transistors,[4] hydrogen sensors,[5] and proton separation.[6]

To date, most studies on proton-conducting CPs have been conducted exclusively on their crystalline or pelletized form.[7] It is known that the introduction of flexibility, namely, excellent mechanical stability against external forces, such as compressive, tensile, and flexural forces into the CPs not only increases feasibility for various applications but also expands the range of their practical use; for example, flexible proton exchange membrane fuel cells offer significant advantages over conventional cells such as mechanical stability, easy integration, and excellent portability.[8] However, the framework structure consisting of directional covalent or coordination bonds poses difficulty in introducing their mechanical flexibility.[9] To overcome this drawback, researchers have utilized low-dimensional CPs with an open-framework structure where each chain or sheet unit is connected by weak van der Waals interactions. The flexural properties of needle-shaped crystalline CPs with one-dimensional (1D) coordination structures have been extensively investigated;[10] however, mechanically flexible crystalline CPs with two-dimensional (2D) coordination structures have been almost unexplored despite their high surface-to-volume ratio, which is potentially beneficial for various applications mentioned above. Although there are several flexible polymer composites embedded with CPs,[11] it is known that the chemical/physical properties of the composites largely depend on the type of polymer and loading amount of CPs.[12] Therefore, the realization of a flexible membrane composed solely of CPs is desirable for the rational design of mechanically flexible proton-conducting CPs and their applications in protonic devices. Furthermore, a key issue in promoting the application of CPs is the stability of their structural and proton-conducting properties during repetitive sequences between flat and bending states; however, there is yet to be a report on the effect of applied external force on the proton conductivity of 2D CPs.

We have focused on proton-conducting 2D CPs composed of tetradentate metal porphyrins and paddlewheel-type metal dimers connected by coordination bonds.[13] Highly flexible behavior, which is a reflection of the layered structure formed by interlayer van der Waals interactions, Cu_2(CuTCPP) (H_4(H_2TCPP); 5,10,15,20-tetrakis(4-carboxyphenyl)porphyrin) membrane was first reported by Xu *et al.*,[13c] whereas our group recently realized an all-solid proton-rectifying device with exceptionally high performance (rectification ratio > 200) using Cu_2(CuTCPP) membrane.[13d] In this study, we investigated the proton-conducting behavior of a highly oriented free-standing membrane of a nickel substituent, Cu_2(NiTCPP), under applied bending stress (Figure S1). Excellent mechanical properties, which were visually manifested with the low limited bending radius, were quantitatively evaluated using bending and tensile stress-strain tests. Our present study is the first to demonstrate that the proton conductivity of a membrane composed solely of CPs remains almost constant during repetitive sequences between flat and bending states, which would be an important step toward the future exploration of mechanically flexible 2D CPs.

Cu_2(NiTCPP) nanosheets were prepared by a stepwise synthesis procedure. H_4(NiTCPP) was prepared by reacting *meso*-tetrakis(4-carboxyphenyl)porphyrin ($H_4(H_2TCPP)$) with $Ni(OAc)_2{\cdot}4H_2O$ according to literature (Supporting Information for details).[14] The successful synthesis of H_4(NiTCPP) was verified by ultraviolet–visible (UV–vis) absorption (Figure S2), Fourier transform infrared (FT-IR) (Figure S3) spectra in addition to ^{1}H nuclear magnetic resonance (NMR) spectra (Figure S4). Purple crystalline Cu_2(NiTCPP) nanosheets were obtained by a solvothermal reaction in *N*,*N*-dimethylformamide, used as a solvent, as previously reported (Supporting Information for details).[13c] The powder X-ray diffraction (XRD) pattern of the pulverized Cu_2(NiTCPP) nanosheets is consistent with the simulated pattern of homobimetallic 2D CP, Cu_2(CuTCPP) (Figure S5) with a layered structure.[13] As shown in Figure 1a, each Cu_2(NiTCPP) sheet has a square grid structure in the *ab* plane, which is composed of tetradentate nickel(II) porphyrin ($NiTCPP^{4-}$) and paddlewheel-type copper(II) dimers. Along the *c* axis, the reticulate layers were assembled mainly through the van der Waals interactions in the AB stacking mode, where the B layer shifted by approximately *a*/4 relative to the A layer. The FT-IR spectra show the disappearance of the peak corresponding to the N−H bending mode (966 cm^{-1} in $H_4(H_2TCPP)$) in H_4(NiTCPP), indicating the metallization of the porphyrin units (Figure 1b). The disappearance of the C=O stretching mode in COOH groups (1676 cm^{-1} in H_4(NiTCPP)) in Cu_2(NiTCPP) confirms that four carboxyl groups of the NiTCPP units successfully coordinated to the adjacent copper ions to form copper paddlewheel units.[15] X-ray photoelectron spectroscopy (XPS) detected peaks of characteristic Cu and Ni atoms in Cu_2(NiTCPP) (Figures 1d and 1e). The peaks at approximately 955 and 935 eV are assigned to Cu $2p_{1/2}$ and Cu $2p_{3/2}$, respectively,[16] whereas those at approximately 873 and 856 eV are assigned to Ni $2p_{1/2}$ and Ni $2p_{3/2}$, respectively.[17] The Cu/Ni molar ratio estimated from the X-ray fluorescence (XRF) analysis (1.9) was consistent with the expected composition. Thermogravimetric analysis indicates that Cu_2(NiTCPP) is thermally stable up to ca. 340 °C (Figure S6). The transmission electron microscope (TEM) image of Cu_2(NiTCPP) deposited onto a carbon-coated copper substrate by dropping ethanol suspension reveals a nanosheet-like morphology (Figure 1c).

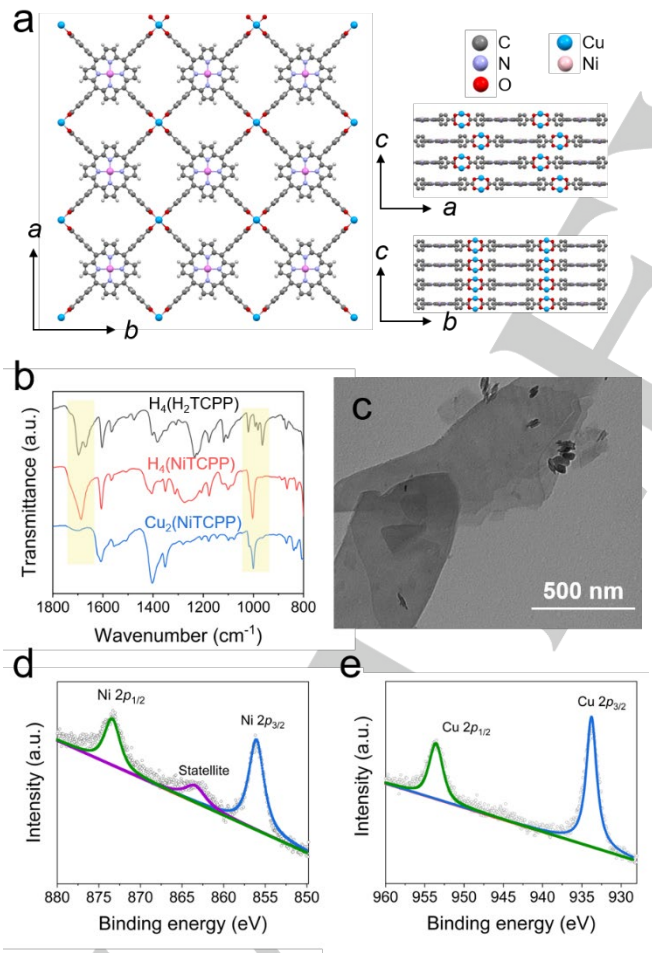

Figure 1. (a) Simulated 2D sheet structure of Cu_2(NiTCPP). (b) Infrared spectra of $H_4(H_2TCPP)$ (black), H_4(NiTCPP) (red), and Cu_2(NiTCPP) (blue). (c) Transmission electron microscope image of Cu_2(NiTCPP) nanosheets. X-ray photoelectron spectra of (d) Ni 2*p* and (e) Cu 2*p* regions in Cu_2(NiTCPP) nanosheets, where the blue, green, and purple lines are fitted to the measured data (open circles).

Owing to the good dispersion of Cu_2(NiTCPP) nanosheets in ethanol, the ethanol suspension was filtered through a polyvinylidene difluoride (PVDF) membrane filter to yield a highly oriented membrane. The membrane with high flexibility could be readily peeled from the filter after drying at 50 °C. Figure 2a shows a photograph of the free-standing membrane with a diameter of 17 mm and a thickness of approximately 8 μm. The thickness can be controlled in the range of less than ten to hundreds of micrometers by adjusting the loading amounts of the suspension. The cross-sectional scanning electron microscope (SEM) image (Figure 2b) shows the membrane formed by stacking nanosheets, which is consistent with the SEM image of the membrane surface (Figure S8). Figure 2c shows the out-of-plane and in-plane grazing incidence XRD patterns of the membranes. The out-of-plane XRD pattern was dominated by the interlayer (002) reflection, indicating the preferred orientation of the membrane along the crystallographic *c*-axis. In the in-plane XRD pattern, all the peaks can be assigned to (*hk*0) reflections because of the highly oriented stacking of nanosheets in the membranes.

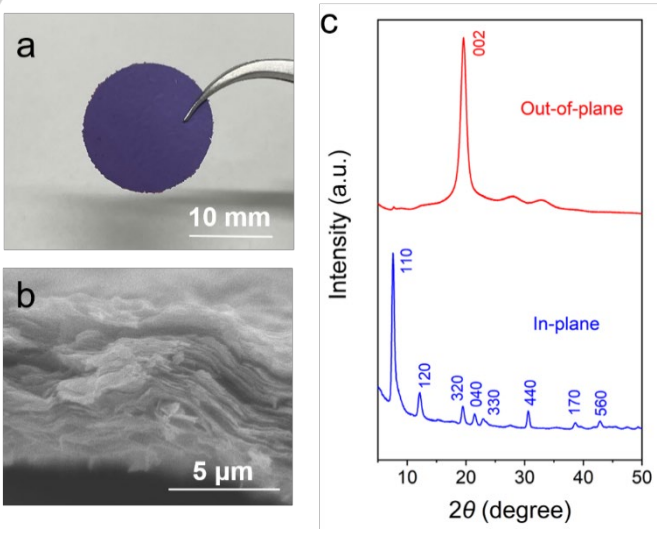

Figure 2. (a) Photograph of Cu_2(NiTCPP) free-standing membrane. (b) Cross-sectional scanning electron microscope image of Cu_2(NiTCPP) membrane. (c) Out-of-plane (red) and in-plane (blue) X-ray diffraction (XRD) patterns of Cu_2(NiTCPP) membrane.

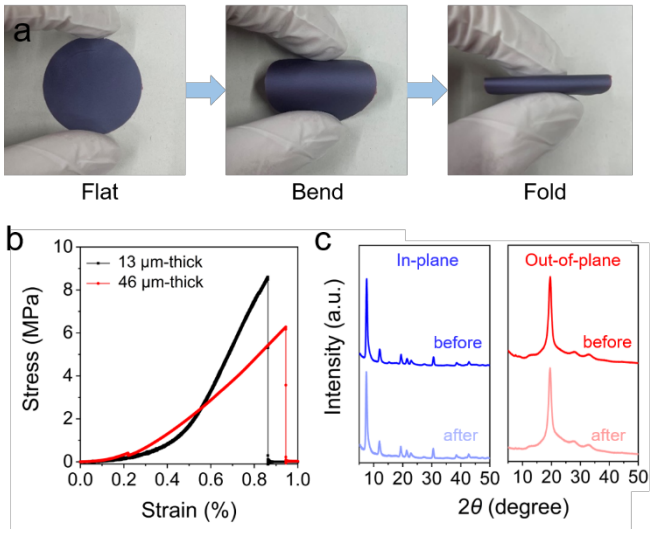

Figure 3. (a) Bending resistance test of Cu_2(NiTCPP) free-standing membrane with a thickness of 8 μm. (b) Tensile stress–strain curves of the membranes with the thickness of 13 μm (black) and 46 μm (red). (c) In-plane and out-of-plane XRD patterns of the membrane before (blue/red) and after (pale blue/pale red) bending, as shown in Figure 3a.

In general, crystalline CPs are highly fragile because of their three-dimensional network formed by directional coordination and covalent bonds.[10d] However, the present Cu_2(NiTCPP) membrane possessed excellent flexibility, possibly because of its 2D layered structure. The limited bending radius (R) of the 8-μm-thick membrane is less than 1 mm (Figures 3a and S9), which is significantly smaller than that of a 500-nm-thick graphene membrane obtained by chemical vapor deposition (R ≈ 2.3 mm).[18] No morphological changes were observed on the surface or cross-section of the membrane after bending and folding (Figure S10), demonstrating that the structure of the membrane is intact against the mechanical stress. Furthermore, we confirmed that the membrane returns to its original flat state after repeated bending and relaxation operations of the membrane at least 20 times (Figure S9) while maintaining the layered structure (Figure S11).

A tensile stress-strain test was performed on the rectangular membrane (Figure S12). As shown in Figure 3b, the curves for the 13-μm and 46-μm-thick membranes exhibit a toe region in the initial stage, possibly arising from the stretching of the wrinkled membrane, followed by a linear elastic behavior until the abrupt fracture. Young's modulus was calculated to be 1.9 and 0.9 GPa for 13-μm-thick and 46-μm-thick membranes, respectively, from the slope of the curve in the linear region, which is higher than those of commercial Nafion membranes (ca. 0.2 GPa).[19] The higher Young's modulus of the thinner membrane can be associated with the less wrinkled or denser structure of its surface layers owing to the surface tension during vacuum filtration. The fracture strength, which is defined as a stress level at the fracture location, of the 13-μm-thick membrane (8.6 MPa) is higher than that of the 46-μm-thick membrane (6.3 MPa). This can be ascribed to the same reason as that of Young's modulus of the membranes, that is, the smaller inter-sheet spacing in the thinner membrane.[20] The fracture strain of the membranes was estimated to be 0.86% and 0.94% for the 13-μm-and 46-μm-thick membranes, respectively. Notably, the Cu_2(NiTCPP) membrane exhibited the same level of mechanical properties (Young's modulus, fracture strength, and fracture strain) as membranes of

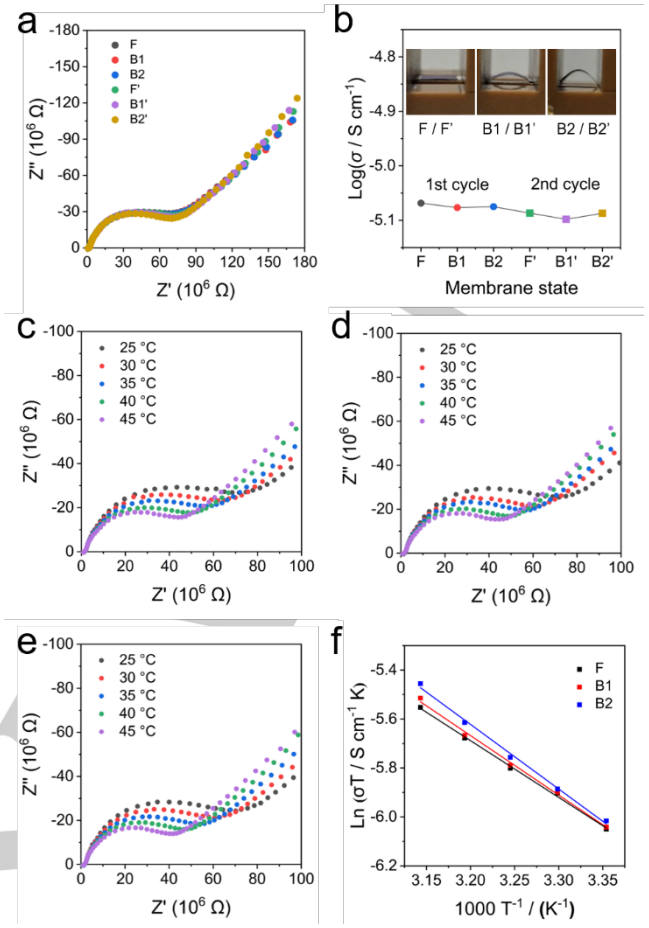

Figure 4. (a) Nyquist plots of Cu_2(NiTCPP) membrane at 25 °C and 98% RH in various bending states; F: flat, B1: 1st bending state (R = 5.3 mm), B2: 2nd bending state (R = 3.8 mm); F', B1', and B2' are equivalent to those of F, B1, and B2, respectively, in the second cycle. (b) Proton conductivity (σ) of Cu_2(NiTCPP) membrane at 25 °C and 98% RH in various bending states (the inset s the photographs of each bending state). Temperature dependence of the Nyquist plots of Cu_2(NiTCPP) membrane in the (c) F, (d) B1, and (e) B2 states at 98% RH. (f) Arrhenius plots of σ of Cu_2(NiTCPP) membrane in various bending states.

typical 2D nanomaterials, such as graphene and WS_2 fabricated by a similar procedure (Table S1).[21]

We also performed a three-point bending test of the 46-μm-thick membrane (Figure S13). Notably, the flexural modulus (approximately 2.8 GPa) was comparable with that of typical commercial polymers, such as polycarbonate (PC), poly(butylene terephthalate) (PBT), poly(ethylene terephthalate) (PET), and poly(ether ether ketone) (PEEK).[22] The structural durability of the membranes against bending and folding was validated by measuring in-plane and out-of-plane XRD patterns, which remained unchanged after the bending operation (Figure 3c).

Room-temperature in-plane proton conductivity (σ) of a Cu_2(NiTCPP) membrane with a thickness of 60 μm was measured using the a.c. impedance method. As shown in Figure S14, the size of the high-frequency semicircle in the Nyquist plot decreased as the relative humidity (RH) increased from 75% RH to 95% RH. Given that the water vapor sorption isotherm shows a steep increase in water uptake above P/P_0 ~ 0.6 (Figure S15), this tendency indicates that the protons originating from the uncoordinated carboxylic groups[23] act as main charge carriers through Grotthuss hopping between the water molecules in the interlayer spacing.

To validate the robustness of proton conductivity against the applied bending stress, the impedance spectra of the membrane formed in a rectangular shape (length: 9.40 mm, width: 5.92 mm, thickness: 35 μm) were measured in three bending states, i.e., flat (F), 1st bending (B1; R = 5.3 mm), and 2nd bending (B2; R = 3.8 mm) (Figure S17). The application of bending stress had minimal effect on the Nyquist plot (Figures 4a and S18); thus, the σ of 8.0 to 8.5 × 10^{-6} S cm^{-1}, as calculated from the semicircle, was comparable regardless of the bending state (Figure 4b). An additional durability test during repetitive sequences between the flat and bending states confirmed the retention of proton conduction (Figure S19). Given that the packing structure in the membrane remained intact during bending, as shown in Figure 3c, the excellent mechanical properties allow to envisage the present membrane for feasible applications as flexible protonic devices.

Figures 4c–4e display the temperature dependence of the Nyquist plots of the membrane in the F, B1, and B2 states, respectively. As expected, the σ value at 25 °C is almost constant under different bending stresses. For all bending states, the σ value steadily increased with increasing temperature and eventually reached 1.2 to 1.3 × 10^{-5} S cm^{-1} at 45 °C in different bending states; namely, their proton conductivities are maintained even under heating. Figure 4f shows the Arrhenius plots for the σT values of the membrane in the three bending states. Each activation energy (E_a) was estimated to be 0.20, 0.21, and 0.23 eV in F, B1, and B2 states, respectively, using the Arrhenius equation given by $\sigma T = A \exp(-E_a/k_B T)$ (A: pre-exponential factor; k_B: Boltzmann constant). The low E_a values suggest that proton conduction is primarily governed by the Grotthuss mechanism,[24] which refers to the proton migration via an infinite network of hydrogen bonds in the conducting medium. Given that the E_a value highly depends on the concentration of the proton species or the distance between proton-hopping sites,[7c] the comparable values confirmed the retention of the proton-conducting pathway under the applied bending stress.

In conclusion, we fabricated highly flexible free-standing membranes composed of 2D CP, Cu_2(NiTCPP). The membrane was highly oriented and had excellent mechanical properties owing to the weak interlayer interactions of van der Waals type. The σ value of the membrane remained almost unchanged even under applied bending stress. The proton-conducting properties and structural features in different bending states strongly indicate that the proton-conducting pathway through the hydrogen bonding network remained intact during bending operation. This is the first study to demonstrate the robust proton conduction of 2D CP against the applied bending stress. The prominent advantage of the present membrane for future flexible protonic devices is that it can be fabricated free from any substrate and shows excellent bending stability even without blending with the polymer matrix. Thus, this study will offer the opportunity to extend the range of feasible applications of CPs in protonic devices.

Acknowledgements

This work was supported by the ACCEL program (JPMJAC1501) of the Japan Science and Technology Agency (JST) and JSPS KAKENHI (Grant Nos. 20H02708 and 20H05623).

Conflict of Interest

The authors declare no conflict of interest.

Data Availability Statement

The data that support the findings of this study are available from the corresponding author upon reasonable request.

Keywords: porous coordination polymer (PCP) • free-standing membrane • high orientation • mechanical flexibility • proton conductivity

[1] a) O. M. Yaghi, M. O'Keeffe, N. W. Ockwig, H. K. Chae, M. Eddaoudi, J. Kim, *Nature* **2003**, *423*, 705–714; b) S. Kitagawa, R. Kitaura, S. I. Noro, *Angew. Chem. Int. Ed.* **2004**, *43*, 2334-2375, *Angew. Chem.* **2004**, *43*, 2334-2375; c) H. C. Zhou, J. R. Long, O. M. Yaghi, *Chem. Rev.* **2012**, *112*, 673-674.

[2] J. Canivet, A. Fateeva, Y. Guo, B. Coasne, D. Farrusseng, *Chem. Soc. Rev.* **2014**, *43*, 5594-5617.

[3] a) Y. Ye, L. Gong, S. Xiang, Z. Zhang, B. Chen, *Adv. Mater.* **2020**, *32*, 1907090; b) S. Paul, S. J. Choi, H. J. Kim, *Energy & Fuels* **2020**, *34*, 10067-10077.

[4] G. D. Wu, H. L. Zhou, Z. H. Fu, W. H. Li, J. W. Xiu, M. S. Yao, Q. H. Li, G. Xu, *Angew. Chem. Int. Ed.* **2021**, *60*, 9931-9935, *Angew. Chem.* **2021**, *133*, 10019-10023.

[5] a) S. Z. Huang, S. S. Liu, H. J. Zhang, Z. Han, G. Zhao, X. Y. Dong, S. Q. Zang, *ACS Appl. Mater. Interfaces* **2020**, *12*, 28720-28726; b) L. D. Costanzo, B. Panunzi, *Molecules* **2021**, *26*, 2952; c) S. L. Yang, G. Li, M. Y. Guo, W. S. Liu, R. Bu, E. Q. Gao, *J. Am. Chem. Soc.* **2021**, *143*, 8838-8848.

[6] a) X. Li, H. Zhang, J. Hou, R. Ou, Y. Zhu, C. Zhao, T. Y. Qian, C. D. Easton, C. Selomulya, M. R. Hill, H. Wang, *J. Am. Chem. Soc.* **2020**, *142*, 9827-9833; b) J. Lu, H. Xu, H. Yu, X. Hu, J. Xia, Y. Zhu, F. C. Wang, H. A. Wu, L. Jiang, H. Wang, *Sci. Adv.* **2022**, *8*, eabl5070.

[7] a.) P. Ramaswamy, N. E. Wong, G. K. Shimizu, *Chem. Soc. Rev.* **2014**, *43*, 5913-5932; b) D. W. Lim, H. Kitagawa, *Chem. Soc. Rev.* **2021**, *50*, 6349-6368.

[8] a) J. Wang, N. He, J. Fei, Z. Ma, Z. Ji, Z. Chen, N. Nie, Y. Huang, *J. Power Sources* **2022**, *551*, 232190; b) Y. Yang, X. Zhu, Q. Wang, D. Ye, R. Chen, Q. Liao, *Appl. Therm. Eng.* **2022**, *203*, 117937.

[9] a) S. Kusumoto, Y. Kim, S. Hayami, *Coord. Chem. Rev.* **475**, *214890*; b) X. Zhou, H. Jin, B. Y. Xia, K. Davey, Y. Zheng, S. Z. Qiao, *Adv. Mater.* **2021**, *33*, 2104341.

[10] a) M. Đaković, M. Borovina, M. Pisačić, C. B. Aakeröy, Ž. Soldin, B. M. Kukovec, I. Kodrin, *Angew. Chem. Int. Ed.* **2018**, *57*, 14801-14805, *Angew. Chem.* **2018**, *130*, 15017-15021; b) M. Pisacic, I. Biljan, I. Kodrin, N. Popov, Z. Soldin, M. Đaković, *Chem. Mater.* **2021**, *33*, 3660-3668; c) B. Bhattacharya, A. A. Michalchuk, D. Silbernagl, M. Rautenberg, T. Schmid, T. Feiler, K. Reimann, A. Ghalgaoui, H. Sturm, B. Paulus, F. Emmerling, *Angew. Chem. Int. Ed.* **2020**, *59*, 5557-5561, *Angew. Chem.* **2020**, *59*, 5557-5561; d) L. C. An, X. Li, Z. G. Li, Q. Li, P. J. Beldon, F. F. Gao, Z. Y. Li, S. Zhu, L. Di, S. Zhao, J. Zhu, D. Comboni, I. Kupenko, W. Li, U. Ramamurty, X. H. Bu, *Nat. Commun.* **2022**, *13*, 6645.

[11] a) J. Yan, T. Liu, X. Liu, Y. Yan, Y. Huang, *Coord. Chem. Rev.* **2022**, *452*, 214300; b) Y. Shi, B. Liang, R. B. Lin, C. Zhang, B. Chen, *Trends Chem.* **2020**, *2*, 254-269; c) F. Jin, F. J. Liu, Y. Chen, Z. Zhang, *Angew. Chem. Int. Ed.* **2021**, *60*, 14222-14235, *Angew. Chem.* **2021**, *133*, 14342-14355.

[12] a) O. Shekhah, J. Liu, R. A. Fischer, C. Wöll, *Chem. Soc. Rev.* **2011**, *40*, 1081-1106; b) J. Dechnik, J. Gascon, C. J. Doonan, C. Janiak, C. J. Sumby, *Angew. Chem. Int. Ed.* **2017**, *56*, 9292-9310, *Angew. Chem.* **2017**, *129*, 9420-9439.

[13] a) G. Xu, T. Yamada, K. Otsubo, S. Sakaida, H. Kitagawa, *J. Am. Chem. Soc.* **2012**, *134*, 16524-16527; b) G. Xu, K. Otsubo, T. Yamada, S. Sakaida, H. Kitagawa, *J. Am. Chem. Soc.* **2013**, *135*, 7438-7441; c) M. Tian, F. Pei, M. Yao, Z. Fu, L. Lin, G. Wu, G. Xu, H. Kitagawa, X. Fang, *Energy Storage Mater.* **2019**, *21*, 14-21; d) J. Lu, Y. Yoshida, M. Maesato,

H. Kitagawa, *Angew. Chem. Int. Ed.* **2022**, *61*, e202213077, *Angew. Chem.* **2022**, *134*, e202213077.

[14] a) G. Granados-Oliveros, E. A. Páez-Mozo, F. M. Ortega, C. Ferronato, J. M. Chovelon, *Appl. Catal. B* **2009**, *89*, 448-454; b) P. K. Sonkar, K. Prakash, M. Yadav, V. Ganesan, M. Sankar, R. Gupta, D. K. Yadav, *J. Mater. Chem.* **2017**, *5*, 6263-6276; c) K. Jeong, J. M. Kim, S. H. Kim, G. Y. Jung, J. Yoo, S. H. Kim, S. K. Kwak, S. Y. Lee, *Adv. Funct. Mater.* **2019**, *29*, 1806937.

[15] R. Makiura, S. Motoyama, Y. Umemura, H. Yamanaka, O. Sakata, H. Kitagawa, *Nat. Mater.* **2010**, *9*, 565-571.

[16] L. Wang, P. Jin, J. Huang, H. She, Q. Wang, *ACS Sustain. Chem. Eng.* **2019**, *7* 15660–15670.

[17] C. Berrios, G. I. Cardenas-Jiron, J. F. Marco, C. Gutierrez, M. S. Ureta-Zanartu, *J. Phys. Chem. A* **2007**, *111*, 2706-2714.

[18] J. Yun, D. Kim, G. Lee, J. S. Ha, *Carbon* **2014**, *79*, 156-164.

[19] M. B. Satterfield, J. B. Benziger, *J. Polym. Sci. B Polym. Phys.* **2009**, *47*, 11-24.

[20] a) A. A. Griffith, *Philos. Trans. R. Soc. London A* **1921**, *221*, 163; b) T. Gong, D. V. Lam, R. Liu, S. Won, Y. Hwangbo, S. Kwon, J. Kim, K. Sun, J. H. Kim, S. M. Lee, C. Lee, *Adv. Funct. Mater.* **2015**, *25*, 3756–3763.

[21] J. N. Coleman, M. Lotya, A. O'Neill, S. D. Bergin, P. J. King, U. Khan, K. Young, A. Gaucher, S. De, R. J. Smith, I. V. Shvets, S. K. Arora, G. Stanton, H.Y. Kim, K. Lee, G. T. Kim, G. S. Duesberg, T. Hallam, J. J. Boland, J. J. Wang, J. F. Donegan, J. C. Grunlan, G. Moriarty, A. Shmeliov, R. J. Nicholls, J. M. Perkins, E. M. Grieveson, K. Theuwissen, D. W. McComb, P. D. Nellist, V. Nicolosi, *Science* **2011**, *331*, 568-571.

[22] K. Van de Velde, P. Kiekens, *Polym. Test.* **2001**, *20*, 885-893.

[23] Y. N. Zhou, L. L. Liu, Q. W. Liu, X. X. Liu, M. Z. Feng, L. Wang, Z. G. Sun, Y. Y. Zhu, X. Zhang, C. Q. Jiao, *Inorg. Chem.* **2021**, *60*, 17303-17314.

[24] D. Marx, *ChemPhysChem* **2006**, *7*, 1848-1870.

Entry for the Table of Contents

Insert graphic for Table of Contents here.

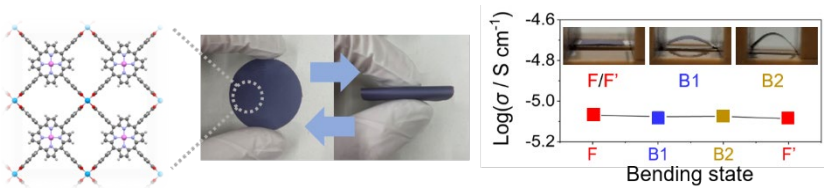

We fabricated a highly oriented free-standing membrane composed of a two-dimensional (2D) coordination polymer (CP) with excellent mechanical properties under stress. This is the first study to demonstrate the robust proton conduction of 2D CPs under an applied bending stress. We found that proton conductivity remained almost constant during bending.